Pure Appl. Chem., Vol. 77, No. 3, pp. 653–665, 2005.
DOI: 10.1351/pac200577030653

Gas–liquid interactions in solution*

M. F. Costa Gomes‡ and A. A. H. Pádua

Laboratoire de Thermodynamique des Solutions et des Polymères, CNRS/Université Blaise Pascal Clermont-Ferrand, 63177 Aubière, France

Abstract: Two approaches are followed to understand how molecular interactions influence the macroscopic properties of solutions: (1) experiment, through the determination of gas solubility, and (2) computer simulation, used to evaluate microscopic properties (structural and energetic). Examples of application of these approaches are considered in order to explain the properties of solutions containing fluorinated fluids or ionic liquids. The molecular structures and interactions are described by force fields built from ab initio quantum chemical calculations. These models allow the determination of free energies from computer simulations by using appropriate energy routes provided by statistical mechanics. The macroscopic properties related to the process of dissolution of several gases are interpreted in terms of the molecular structure of the solutions and of the solute–solvent interactions.

Keywords: solubility; molecular simulation; gas; fluorinated liquids; ionic liquids.

INTRODUCTION

Gas–liquid interactions determine the physicochemical behavior of solutions that are important to a variety of fields, ranging from medicine to chemical technology. In order to understand how solutes interact with solvents and how these molecular forces influence the macroscopic properties of the solutions, two approaches can be followed: (1) experiment, with the study of the thermodynamics of solution, and (2) molecular simulation, used to evaluate microscopic properties both structural and energetic.

The thermodynamic properties of solvation can be determined from the variation of the solubility with temperature. Henry's law constants, calculated from gas solubility data, can be exactly converted to the Gibbs energy of solvation, a quantity that corresponds to the change in partial molar Gibbs energy when the solute is transferred, at constant temperature, from the pure perfect gas at standard pressure to the infinitely dilute state in the solvent. For the case of gaseous solutes at low pressure, this free energy of solvation can be regarded as a reasonable approximation for the Gibbs energy of solution. Solubility measurements often constitute a valuable source of information about the properties of the solutions, especially in the case of very dilute solutes for which direct calorimetric determinations are very difficult. Furthermore, the Gibbs energy of solvation is accessible by models of statistical thermodynamics and can be directly calculated by molecular simulation provided a realistic intermolecular force field is available.

Molecular simulations become an increasingly common means of elucidating the structure and predicting the properties of solutions. Continuing growth in computing power makes it possible to consider more complex systems, modeled by increasingly detailed force fields. For example, it is now usual

*Paper based on a presentation at the 11th International Symposium on Solubility Phenomena (11th ISSP), Aveiro, Portugal, 25–29 July 2004. Other presentations are published in this issue, pp. 513–665.

‡Corresponding author

to describe the intra- and intermolecular interactions using all atoms explicitly rather than using a simpler united-atom approach. Moreover, parameterization of the intramolecular features of the models can be done with more sophisticated (and accurate) ab initio quantum mechanical treatments. The intermolecular terms, on the other hand, are still reduced from fluid-phase properties considering, when possible, several species within a homologous family. Interactions between different molecular types are seldom taken into account and so it is difficult to foresee how a particular force field would describe the properties of mixtures. Well-chosen experimental data of high accuracy on properties evidencing the role of unlike interactions provide a route to verify and, when necessary, improve this description. Dilute solutions are convenient systems to study when pursuing this goal as the solute–solute interactions are absent and the focus lies on the solute–solvent interactions.

The present paper describes two examples in which a double approach, experiment and molecular simulation, has served to explain the macroscopic thermodynamic properties of solutions at a molecular level. These examples concern gaseous solutes in liquid fluorinated solvents and in ionic liquids.

METHODS

In this section, the two methods used to assess the influence of molecular interactions in the macroscopic properties of solutions are described. First, the main features of the experimental techniques employed to measure gas solubility as a function of temperature are described. A series of experimental procedures, each with different characteristics, are used to study the solutions of gases. Second, the theoretical methods, based on statistical mechanics, employed for the interpretation of the results are explained at the end of this section.

Experiments

Low-pressure gas solubility can be measured experimentally using several instruments working on the basis of pressure–volume–temperature–composition (p,V,T,x) determinations. The available techniques were developed taking into account different characteristics of the solvents studied (vapor pressure, viscosity, surface tension, etc.) and aiming at distinct levels of precision and accuracy on the gas solubility.

A block diagram describing the general procedure of this type of gas solubility experiments is shown in Fig. 1. A number of different experimental apparatuses are briefly described.

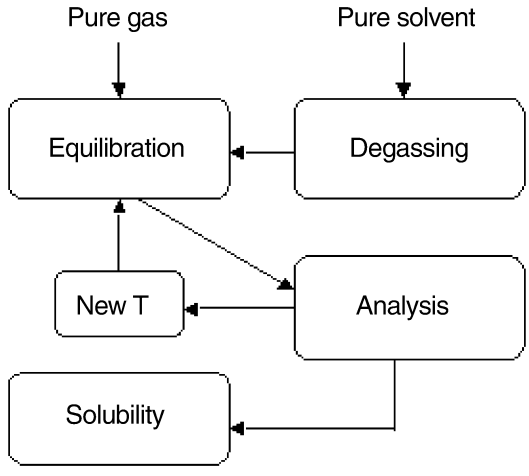

Fig. 1 Block diagram of the experimental determination of gas solubility at low pressures.

In the extraction technique [1,2], the solubility of a gaseous solute in a liquid solvent is determined by quantitatively extracting the gas from the previously saturated solution at a given temperature and pressure. The first step consists in degassing the solvent, which is then put in contact with the gas for equilibration in a specially designed equilibrium cell [3]. When thermodynamic equilibrium is reached, gas- and liquid-phase samples of precisely known volumes are isolated. The amount of dry gas present in each sample is precisely quantified by a (p,V,T) analysis.

This technique offers the highest precision obtained so far with (p,V,T,x) methods. It requires a large volume of solvent, and measurements are time-consuming (equilibration times of 24 to 48 h). It is, therefore, a technique appropriate for reference work on simple systems. The uncertainty in solubility, expressed as Henry's law constant, was found to be lower than 0.1 % for several aqueous solutions.

The isobaric saturation method was originally developed by Ben-Naim and Baer [4] and was the object of several modifications, including the automation of the experimental apparatus [5] and the elimination of mercury [6,7]. This technique offers the advantages of shorter measurement times and smaller sample sizes. It is also simpler in instrumental terms, and its operation is easier when compared to the extraction method. The uncertainties obtained are still below 1 % in solubility.

In this case, a known amount of pure solvent is transferred into a saturation cell [8], filling it up to a level in capillary tubes. The solute gas, presaturated in solvent, is then introduced into the apparatus. Recirculation of the solvent through the capillaries promotes a large gas–liquid contact surface and enables the dissolution of the gas. Pressure is maintained in the apparatus by displacement of a piston in a glass cylinder containing the gas phase. Once the system attains equilibrium, the amount of gas dissolved is calculated from the volume displaced by the piston. Automation of this type of apparatus is possible through a control loop that maintains the pressure by actuating a motor to displace the piston [5].

An isochoric version of the saturation method has been used to measure gas solubility in a number of systems, requiring even smaller volumes of solvent when compared to the isobaric method and having no mobile parts [9]. In this case, known amounts of dry gas, determined by a (p,V,T) measurement, and liquid solvent, determined gravimetrically, are put in contact at constant temperature. The equilibrium pressure is in direct relation with the gas solubility, provided the saturation properties of the pure solvent are known. The temperature can very easily be changed, and a new state point is obtained when a constant pressure value is attained (indicating that thermodynamic equilibrium at the new temperature is reached). Equilibration times are longer than in the isobaric method, especially with volatile solvents, for an uncertainty that is similarly below 1 %. This technique can be easily extended to the study of mixtures of solvents. In this case, the vapor pressure of the mixture needs to be determined before the gas is put in contact with the liquids and the gas/liquid equilibrium has been attained.

Modeling

Atomistic simulation is the tool of choice to interpret the solubility and derived thermodynamic properties that depend on the structure and interactions at a molecular scale. Application of molecular simulation to solubility phenomena in dilute solutions, and solutions of gases normally fall under this category, requires two elements: the solvent–solvent and solute–solvent interactions have to be specified in a force field; and techniques (routes) to calculate free energies from simulation have to be implemented. The free energy of solvation can be obtained directly from molecular simulation, and related to the solubility through Henry's law constant.

Classical force fields of OPLS-AA/Amber [11,12] type can be used to describe the interactions in solution. These force fields contain parameters for many families of organic molecules. Their functional form contains in general four kinds of potential energy: covalent bond stretching (between every two bonded atoms), valence angle bending (between every three atoms connected by two bonds), dihedral angle torsions (between every four atoms connected by three bonds), and nonbonded interactions. The nonbonded interactions are exerted between atoms of different molecules, and also between atoms

of the same molecule separated by more than three bonds. The potential energy associated with bonds and angles is usually described by harmonic terms. Dihedral torsion energy surfaces are usually rendered by cosine series. Nonbonded terms are commonly given by the Lennard-Jones 12-6 repulsive-dispersive potential complemented with electrostatic terms constituted by point partial charges placed on the atomic sites. Small molecular species such as water and gases are also described in the literature in terms of "Lennard-Jones plus charges" models [12–14].

In spite of the large body of literature on force fields, more often than not some terms necessary to describe certain functional groups, or arrangements of such groups within molecules, are missing, not allowing immediate application of the simulation approach to the system under study. Development of some force field terms, most frequently torsion energy profiles and partial charges, may be necessary in these cases. Nowadays, such tasks of force field development can be accomplished using ab initio quantum chemical tools available in the major software packages. The intermolecular terms, i.e., the Lennard-Jones potential parameters, can be best defined from fits to experimental thermodynamic properties such as densities and heats of vaporization.

Calculation of the chemical potential of the solute requires two steps: firstly, a representative sample of molecular configurations of the liquid solvent (either a pure substance or a mixture) have to be generated; secondly, the chemical potential of the solute in the solvent needs to be evaluated. Generation of the configurations can be accomplished by straightforward simulation using Monte Carlo or molecular dynamics. A sufficient number of molecules has to be used in the simulation box, and sufficient snapshots have to be stored in order to effectively sample the configurational space of the solvent. Then, an appropriate route to the free energy of the solute must be followed, and its choice depends on the characteristics of the system.

The case is simplest for small, nonpolar solutes that interact weakly with the solvent. If the solute is small enough so that cavities capable of hosting one of its molecules can be spontaneously generated in the solvent (with sufficient probability), then direct test-particle insertion [15] can be adopted. This method consists of trying to repeatedly insert the solute molecule in each configuration of the liquid solvent. The residual chemical potential of the solute, which corresponds to the transfer of one solute molecule from the ideal gas state (at the same temperature and density as those of the solution) into the solution, and is therefore analogous to the free energy of solvation, is given by,

$$\Delta G_{\mathrm{solv}} = -kT \frac{\left\langle V \exp\left(-u/kT\right)\right\rangle_{N,p,T}}{\left\langle V\right\rangle_{N,p,T}} \tag{1}$$

where u is the interaction energy of the test particle with a configuration of solvent molecules, V is the volume of the solvent in a given configuration and $\langle\ldots\rangle_{N,p,T}$ denotes an isothermal-isobaric ensemble average.

Henry's law constant is directly related to the free energy of solvation,

$$K_{\mathrm{H}}\left(p,T\right) = RT\rho_1 \exp\left(\frac{\Delta G_{\mathrm{solv}}}{RT}\right) \tag{2}$$

where ρ_1 is the density of the pure solvent, which is equal to that of the solution in the limit of infinite dilution.

In situations where the solute is small enough, but there is strong association with the solvent, giving rise to local order effects, then sampling through test-particle insertion will be statistically poor, since the solvent does not "feel" the solute and its molecules cannot reorganize themselves around it.

For larger or strongly interacting solutes, stepwise insertion methods provide routes to obtain the free energy of solvation in which the solute molecule is created step by step [16], allowing the solvent to respond to the presence of the solute and reorganize itself. The gradual activation of the solute in the

solution can be accomplished through the introduction of an activation parameter, λ, which varies between 0 and 1. The value $\lambda = 0$ corresponds to the absence of solute (initial system), the value $\lambda = 1$ corresponds to the presence of the solute with full interactions (final system). Then, a reversible thermodynamic path has to be created joining the initial to the final systems. For example, the potential energy of solute–solvent interaction can be written depending linearly on the activation parameter,

$$U(\lambda) = \lambda U_B + (1 - \lambda)U_A \tag{3}$$

The free-energy difference between the initial and final systems can be obtained from its expression in terms of the energy of the simulated system.

One way of calculating the free-energy difference upon activation of one solute molecule is the thermodynamic integration (TI) technique [17]. Here, a number of independent simulations is performed, each at a different value of the activation parameter, say every $\Delta\lambda = 0.1$ (giving 11 simulations to perform). Then the integral allowing the calculation of ΔG can be approximated by a numerical formula such as the trapeze or Simpson's rule. One good point about TI is that the simulations are independent and more can be done in regions where the integrand is more tortuous, without losing the work already done. One disadvantage of TI when applied to the problem of calculating free energies of solvation at low concentrations is that the overall energy of the system is rather insensitive to differences in solute–solvent interactions, which are hidden in the "noise" of the solvent molecules interacting with each other.

Another approach is the free-energy perturbation (FEP) method [16]. Suppose the system containing one partially activated solute molecule has been simulated at a particular value of the parameter λ, and that a large number of molecular configurations has been stored (the reference system). Using the same coordinates for all the atoms, the energy of the system in each one of the configurations can be recalculated using the next value of the activation parameter, $\lambda + \Delta\lambda$ (the perturbed system). The free-energy difference resulting from this perturbation is given by,

$$\Delta G = \sum_i -kT \ln \left\langle \exp\left(-\frac{U_{\lambda+\Delta\lambda} - U_\lambda}{kT} \right) \right\rangle_\lambda \tag{4}$$

Of course, in order to check against hysteresis problems, the values of the free energy obtained when going up in λ should be compared with those obtained when coming down. Significant differences indicate that the step chosen is too large, and additional simulations and perturbations would have to be performed. Hysteresis is a frequent problem, and a large number of steps are often required to create a solute molecule starting from the pure solvent. The FEP technique presents a good sensitivity to the fact that only one perturbed solute molecule is present among a large number of solvent molecules, since only the solute–solvent interaction energies that are affected by the activation parameter appear in the difference in eq. 4.

A method that combines the advantages of TI with those of FEP is the finite-difference thermodynamic integration (FDTI) [18]. Here, one proceeds as in the TI method, calculating the free-energy difference by integration,

$$\Delta G = \int_0^1 \frac{\partial G}{\partial \lambda} d\lambda \approx \sum_i w_i \left.\frac{\partial G}{\partial \lambda}\right|_{\lambda_i} \Delta\lambda \tag{5}$$

Only now, the derivative with respect to the activation parameter is calculated by numerical differentiation, that is, approximated by a difference over a small interval $\delta\lambda$,

$$\left.\frac{\partial G}{\partial \lambda}\right|_{\lambda_i} \approx \frac{\left(G_{\lambda+\delta\lambda} - G_\lambda\right) - \left(G_\lambda - G_{\lambda-\delta\lambda}\right)}{2\delta\lambda} \tag{6}$$

Typically, this interval is of the order of 0.001, orders of magnitude smaller than the interval between activation steps $\Delta\lambda$. Therefore, the small free-energy differences which are required to calculate the numerical derivative can be obtained using the FEP method with no risk of hysteresis, and benefiting from its good sensitivity when in the presence of only one solute molecule.

$$\delta_{\pm}G = -kT \ln \left\langle \exp\left(-\frac{U_{\lambda+\delta\lambda} - U_{\lambda}}{kT} \right) \right\rangle_{\lambda} \tag{7}$$

EXAMPLES OF APPLICATION

Applications of the methodologies presented above are applied to the study of two types of solutions. The objective is to explain the macroscopic properties of solution measured experimentally at the level of the molecular interactions.

Solute–solvent interactions in fluorinated solvents

Most gases are highly soluble in fluorinated liquids when compared to other solvents, prompting applications in chemistry, as reaction and extraction media, and in pharmacology, as respiratory gas carriers. The approach outlined above, combining thermodynamic measurements with molecular simulation, has been applied to investigate the reasons why fluorinated liquids dissolve large quantities of gases, and in particular why carbon dioxide is so much soluble in these fluids.

The first step involved a comparison of the structure of a liquid phase of pure fluorinated hydrocarbon with that of the analogous alkane. The torsion energy profiles associated with rotation around a C–C bond in both *n*-hexane and perfluoro-*n*-hexane are shown in Fig. 2.

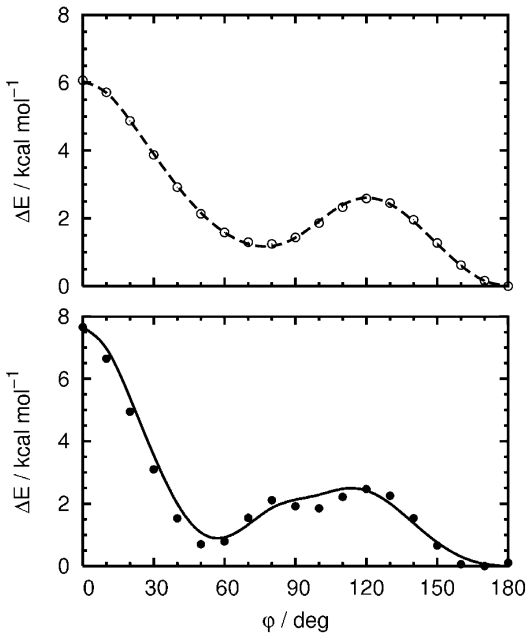

Fig. 2 Torsion energy profiles associated with rotation around C–C bonds in a linear hydrocarbon (upper plot) and perfluorocarbon (lower plot), obtained from ab initio quantum chemical calculations (symbols) and reproduced by molecular simulation (lines). Details of the calculations can be found elsewhere [19].

Some differences are noteworthy. In the perfluorocarbon, the rotation barrier is higher and the most stable conformer does not correspond exactly to a dihedral angle of 180° (trans), but to one of about 170° instead. These two aspects lead to the hypothesis that, in the liquid phase, the perfluorocarbon would have a more rigid carbon backbone than the equivalent hydrocarbon. In a hydrocarbon, the carbon skeleton should present a succession of trans dihedrals with the occasional gauche defect (dihedral angle of about 60° corresponding to the local minimum in the torsion energy). In the perfluorocarbon, the backbone should have a helical form, punctuated by the occasional gauche defect.

In view of this direct observation obtained from molecular simulation, it is expected that larger cavities should be present spontaneously in a liquid perfluorocarbon than in the corresponding hydrocarbon at the same temperature and pressure. Computer simulations of *n*-hexane and perfluoro-*n*-hexane have demonstrated that this prediction is correct [19]. From the population of cavities, it is possible to calculate the free energy of cavity formation in a liquid, that is, the reversible work required to create a cavity of a given size. Free energies of cavity formation in different liquids are plotted in Fig. 3. It is observed that, from all the liquids studied (a hydrocarbon, two fluorinated solvents, and water) it is the perfluorinated liquid that has a lower free energy of cavity formation, an observation coherent with the fact that it is the same species that has a larger population of cavities of any size.

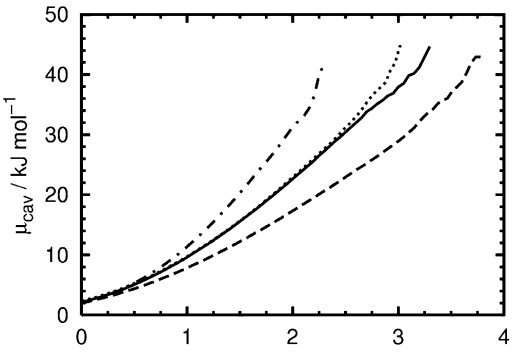

Fig. 3 Free energy of cavity formation calculated by molecular simulation at 300 K and 1 bar in water (–·–), perfluorooctylbromide (····), *n*-hexane (—), and perfluoro-*n*-hexane (– – –).

The solvation process can be thought of as decomposed in two steps: the first consisting of the formation of a cavity in the solvent capable of hosting a solute molecule, and the second being the activation of solute–solvent interactions. Therefore, the lower free energy of cavity formation obtained in the perfluorinated liquid indicates that, for equivalent strength of the interactions, any gas would be more soluble in this medium. This general behavior is corroborated by experiment.

The solubility of different molecules in *n*-hexane and perfluoro-*n*-hexane has been calculated by simulation, in order to compare the effect of the solute–solvent interactions. Oxygen, carbon dioxide, and water have been studied in detail [19], since these provide examples of nonpolar, quadrupolar. and dipolar solutes of major interest for applications of the fluorinated liquids. Carbon dioxide is a larger molecule than oxygen, but is much more soluble in fluorinated phases than the latter gas, as can be seen in Table 1.

The results of solubility calculated by simulation agree with the experimental values within 20 %, which is normal for a pure prediction using interaction models that were not parameterized specifically for the unlike solute–solvent interactions studied here.

It is interesting to see that, removing the electrostatic part from the model of carbon dioxide, that is, removing the quadrupole, the solubility remains very close to that of the original carbon dioxide model. By means of this exercise, it was possible to show [19] that the preponderant term dictating the high affinity between carbon dioxide and fluorinated liquids is not electrostatic in nature, but depends instead on the strength of the dispersive forces. The same observation is valid when analyzing the sol-

Table 1 Solvation free energy and mole fraction solubility of oxygen and of carbon dioxide in *n*-hexane and in perfluoro-*n*-hexane close to atmospheric pressure. The values were determined by molecular simulation.

T/K	ΔG_{solv}/kJmol^{-1}	$x_2/10^{-3}$	ΔG_{solv}/kJmol^{-1}	$x_2/10^{-3}$
		C_6H_{14}		
	O_2		CO_2	
300	1.46	3.0	−2.80	16.6
400	1.54	3.1	−1.54	7.9
		C_6F_{14}		
	O_2		CO_2	
300	1.07	5.4	−2.69	24.3
400	1.40	5.1	−1.21	11.2

ubility of the same solutes in a liquid hydrocarbon: again, carbon dioxide is more soluble than oxygen and removing the electrostatic part does not change the results significantly.

Solute–solvent interactions in ionic liquids

Ionic liquids are organic salts that are molten at room temperature. They form a novel class of solvents with potential industrial applications in environmentally acceptable processes. Ionic liquids can be synthesized in numerous combinations of cation-anion, yielding a vast universe of compounds whose properties are difficult to estimate using macroscopic thermodynamic models. The approach based on the use of a molecular force field to predict macroscopic properties is promising in this case, since it relies on a physicochemical model whose parameters are defined at a more fundamental level than in macroscopic solution theories.

The same strategy presented above for the study of fluorinated liquid phases has been followed in the case of ionic liquids. Their use as solvents in chemical processes implies that their interactions with several gases, including carbon dioxide, are of importance. The novelty of ionic liquids means that the microscopic structures of their solutions are still not well known and molecular simulation offers the opportunity to access it relatively easily.

In Fig. 4, the solubility of several gases in common ionic liquids, 1-butyl-3-methylimidazolium terafluoroborate [bmim][BF_4] and 1-butyl-3-methylimidazolium hexafluorophosphate [bmim][PF_6], calculated by simulation are compared with experiment. This comparison serves to validate the force field. In this case, only qualitative agreement is attained, the order of solubility of the different gases being correctly predicted. Quantitatively, the simulated solubility values are systematically below the experimental data. For some gases, namely nitrogen that has a low solubility in these ionic liquids, experimental data are still controversial. Simulation also predicts that all gases studied are more soluble in [bmim][PF_6] than in [bmim][BF_4]. As in the fluorinated solution, carbon dioxide is much more soluble than the remaining gases, although it has one of the largest molecular sizes. This result prompted an investigation using the same tools as before.

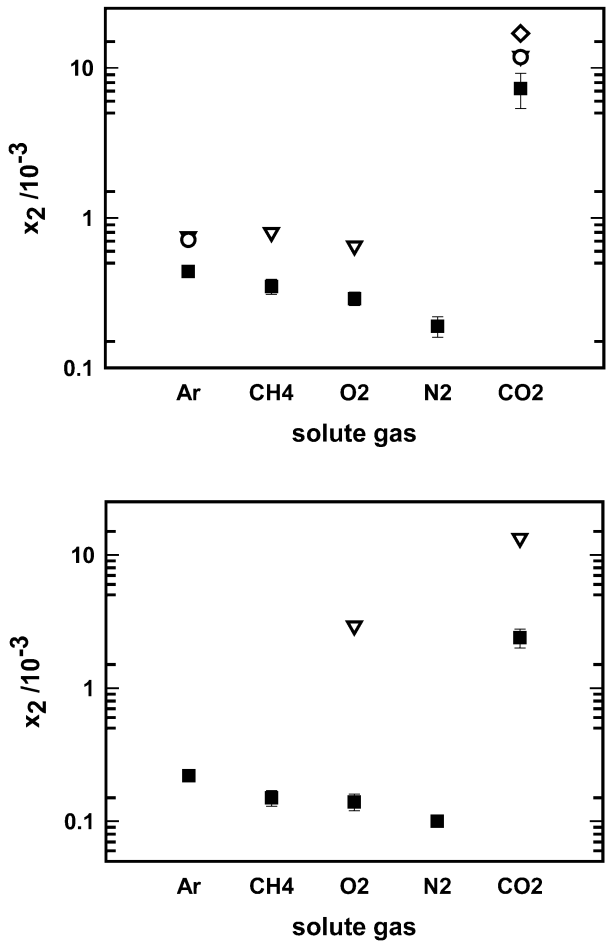

Fig. 4 Solubility of some gases at 1 bar and 323 K in: [bmim][PF_6] (upper plot): ■, simulation; ◇, Anthony et al., 2001 [21]; ▽, Anthony et al., 2002 [22]; ○, Costa Gomes et al., 2004 [23]; [bmim][BF_4] (lower plot): ■, simulation; ▽, Husson-Borg et al., 2003 [24].

The distribution of spontaneous cavity sizes and the associated free energy of cavity formation in the ionic liquids are plotted in Fig. 5. Although these properties have similar values for the two ionic liquids, it is observed that natural cavities are slightly more easily formed in [bmim][PF_6].

The solubility of carbon dioxide in the two ionic liquids is much larger than that of nitrogen and can be calculated accurately by molecular simulation [25]. Removing the electrostatic terms from the carbon dioxide molecular interaction model causes a marked decrease in the solubility indicating that electrostatics play this time a major role in the interactions between carbon dioxide and the ionic liquids. Nitrogen possesses a quadrupole moment of about a quarter of that of carbon dioxide, but curiously, for nitrogen, including or not electrostatic terms in the interaction model does not modify the solubility significantly.

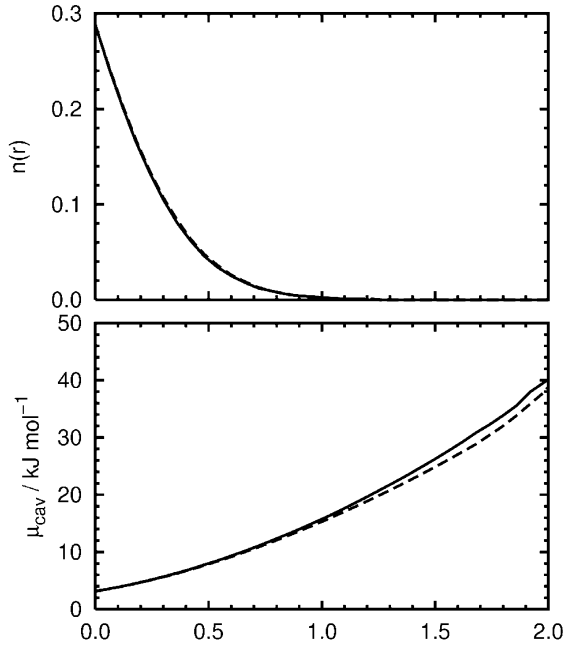

Fig. 5 Distribution of the population of spontaneous cavities (upper plot) and free energy of cavity formation (lower plot) in [bmim][BF_4] (solid line) and in [bmim][PF_6] (dashed line) at 1 bar.

These energetic aspects of the interactions can be complemented in a very useful manner by providing details of the structure of the solution, in the form of site–site radial distribution functions of the solvent atoms around the solute atoms. Such radial distribution functions obtained by simulation are shown in Fig. 6. It can be deduced that carbon dioxide is solvated near C4 and C5, since these functions have maxima at short distance and show intercalated peaks of the oxygen atoms and of the carbon atom (the longitudinal axis of carbon dioxide points toward these carbon atoms of the imidazolium ring). Carbon dioxide is not interacting strongly with the C2 carbon of the imidazolium ring (the carbon bridging the two nitrogen atoms), as would be expected due to the acidic nature of the hydrogen connected to C2.

The radial distribution functions of the phosphorous atoms around carbon dioxide have coinciding first peaks for carbon and for oxygen, indicating the carbon dioxide molecule lies flat against the anion.

As demonstrated in Fig. 7, removing the charges from the carbon dioxide model totally modifies the aspect of the solute–solvent radial distribution functions. The strong orientational order of the functions in Fig. 6 is lost, an observation compatible with a larger rotational freedom of carbon dioxide.

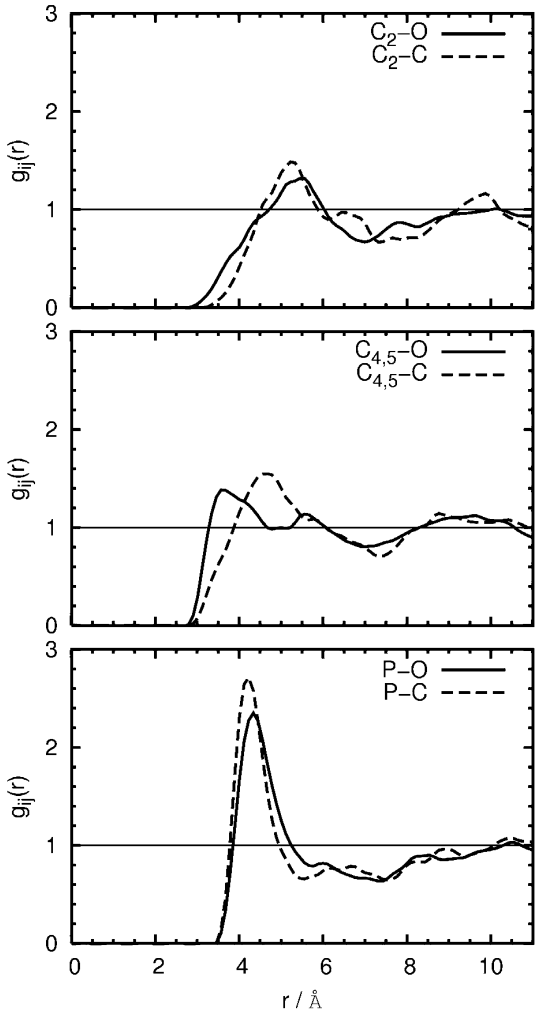

Fig. 6 Site–site solute–solvent radial distribution functions of carbon dioxide in [bmim][PF_6] at 300 K and 1 bar.

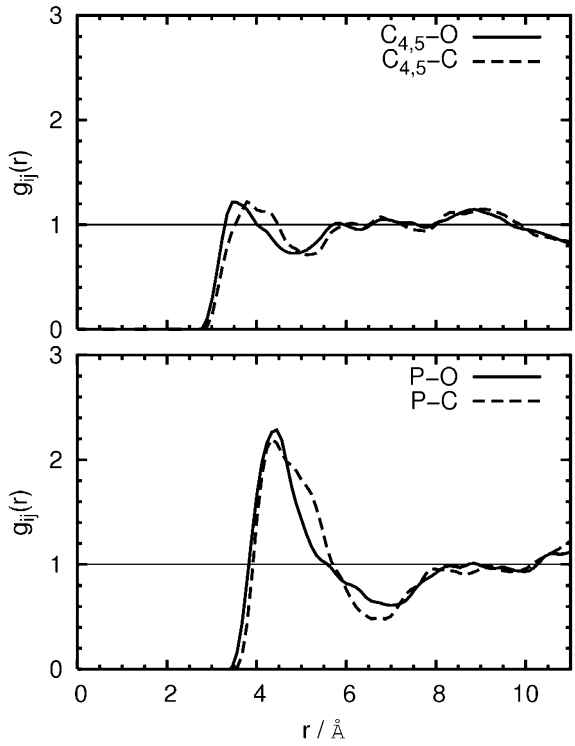

Fig. 7 Site–site solute–solvent radial distribution functions of the carbon dioxide model without electrostatic charges in [bmim][PF_6] at 300 K and 1 bar.

CONCLUSION

Gas-solubility measurements, performed as a function of temperature, allow the derivation of thermodynamic properties of solvation such as free energy and enthalpy. The solubility results permit the validation of molecular force fields that attempt to describe the solute–solvent interactions in solution.

Molecular simulation can be used to calculate the solvation properties starting from a specification of the molecular structure and interactions of the chemical species present in the system. Predictive simulation tools can be used to complement experiments whenever these are too difficult, for example, when solubility is very low or when working conditions involve extreme temperatures or high pressure. Calculation of solubility can be achieved for gaseous solutes and, with a slightly different procedure, also for solutes that exist in the form of condensed phases at standard conditions [20].

The molecular mechanisms determining the dissolution process can be investigated by simulation by isolating the effect of different terms in the interactions. The structure of the solution, concerning the arrangement of the solvation shells around the solute, can be predicted by simulation, even in systems where the low concentration of solute precludes obtaining diffraction data.

REFERENCES

1. M. F. Costa Gomes and J.-P. Grolier. *Phys. Chem. Chem. Phys.* **3**, 1047 (2001).
2. R. P. Bonifacio, A. A. H. Padua, M. F. Costa Gomes. *J. Phys. Chem. B* **105**, 8403 (2001).
3. B. B. Benson, D. Krause, Jr., M. A. Peterson. *J. Solution Chem.* **8**, 655 (1979).
4. A. Ben Naim and S. Baer. *Trans. Faraday Soc.* **59**, 2735 (1963).
5. B. M. Moudgil, P. Somasundaran, I. J. Lin. *Rev. Sci. Instrum.* **45**, 406 (1974).
6. T. Tominaga, R. Battino, H. K. Gorowara, R. D. Dixon, E. Wilhelm. *J. Chem. Eng. Data* **31**, 175 (1986).
7. A. M. A. Dias, R. P. Bonifacio, I. M. Marrucho, A. A. H. Padua, M. F. Costa Gomes. *Phys. Chem. Chem. Phys.* **5**, 543 (2003).
8. J. Carnicer, F. Gibanel, J. S. Urieta, C. Gutierrez Losa. *Rev. Acad. Ciencias Zaragoza* **34**, 115 (1979).
9. R. P. Bonifacio, M. F. Costa Gomes, E. J. M. Filipe. *Fluid Phase Equilib.* **193**, 41 (2002).
10. W. L. Jorgensen, D. S. Maxwell, J. Tirado-Rives. *J. Am. Chem. Soc.* **118**, 11225 (1996).
11. W. D. Cornell, P. Cieplak, C. I. Bayly, I. R. Gould, K. M. Merz, D. M. Ferguson, D. C. Spellmeyer, T. Fox, J. W. Caldwell, P. A. Kollman. *J. Am. Chem. Soc.* **117**, 5179 (1995).
12. Y. Miyano. *Fluid Phase Equilib.* **158–160**, 29 (1999).
13. M. Mahoney and W. L. Jorgensen. *J. Chem. Phys.* **112**, 8910 (2000).
14. J. G. Harris and K. H. Yung. *J. Phys. Chem.* **99**, 12021 (1995).
15. B. Widom. *J. Chem. Phys.* **39**, 2808 (1963).
16. P. Kollman. *Chem. Rev.* **93**, 2395 (1993).
17. D. Frenkel and B. Smit. *Understanding Molecular Simulation*, Academic Press, San Diego (1996).
18. M. Mezei. *J. Chem. Phys.* **86**, 7084 (1987).
19. M. F. Costa Gomes and A. A. H. Pádua. *J. Phys. Chem. B* **107**, 14020 (2003).
20. J. Deschamps, M. F. Costa Gomes, A. A. H. Pádua. *J. Fluorine Chem.* **125**, 409 (2004).
21. J. L. Anthony, E. J. Maginn, J. F. Brennecke. *J. Phys. Chem. B* **105**, 10942 (2001).
22. J. L. Anthony, E. J. Maginn, J. F. Brennecke. *J. Phys. Chem. B* **106**, 7315 (2002).
23. M. F. Costa Gomes, P. Husson, J. Jacquemin, V. Majer. Chapter 16: "Interactions of gases with ionic liquids: Experimental approach", in *Ionic Liquids III: Fundamentals, Progress, Challenges, and Opportunities,* ACS Symposium Series, R. D. Rogers and K. R. Seddon (Eds.), American Chemical Society, Washington DC (2005).
24. P. Husson-Borg, V. Majer, M. F. Costa Gomes. *J. Chem. Eng. Data* **48**, 480 (2003).
25. J. Deschamps, M. F. Costa Gomes, A. A. H. Pádua. *ChemPhysChem* **5**, 1049 (2004).